P. Adnani

I. Catton

M. A. Abdou

Mechanical, Aerospace, and Nuclear Engineering Department, University of California, Los Angeles, Los Angeles, CA 90024

Non-Darcian Forced Convection in Porous Media With Anisotropic Dispersion

Convective heat transfer in a particle packed tube is modeled in this paper. Axial and radial dispersion are both included in the governing equations. Results are compared with experimental data, and with previously developed models that did not include axial dispersion. It is shown that heat transfer in the thermally developing region is affected by axial dispersion when Peclet number is smaller than 10. Graphic results are provided to show the importance of axial dispersion for various Peclet numbers.

Introduction

Forced convection heat transfer in a particle packed tube is of great importance in the design of catalytic reactors and packed particle heat exchangers. Experimental data for flow in packed beds of spheres (Yagi and Wakao, 1959; Kwong and Smith, 1957; Plautz and Johnstone, 1955; Yagi and Kunii, 1960), and packed cylinders (Bunnell et al., 1949; Coberly and Marshall, 1951) are available for a wide range of flow rates and material properties. Some of these authors have also attempted to formulate a mathematical model for this problem by assuming slug flow and uniform thermal conductivity across the tube. These restrictive assumptions were shown some time ago to be invalid. (see Vafai, 1984).

Recent analyses of this problem by Cheng and Vortmeyer (1988) and Hunt and Tien (1988) have focused on the impact of non-Darcian effects on heat transfer. These non-Darcian effects include: (1) porosity variation near solid boundaries, (2) inertial forces in the momentum equation, (3) local dependence of effective medium conductivity on the superficial velocity, and (4) damping of hydrodynamic dispersion near solid boundaries. The existence of these effects in porous media has been verified to a certain extent by various experimental data.

While incorporation of non-Darcian effects in the governing equations has greatly improved the porous media models in the past few years, these models still do not account for all of the physical phenomena that exist in porous media. Our objective here is to look at one of these effects: the importance of axial dispersion. Previous models have always neglected the axial dispersion because the advective term in the axial direction have always been assumed to be larger than the axial dispersion term in this direction. It should be noted that the effective medium conductivity in porous media has two separate components: (1) a stagnant component that represents the medium conductivity when the fluid is not moving, and (2) a dispersive component that depends on the fluid superficial velocity. Therefore, neglecting the axial dispersion may not yield correct results at all Peclet numbers.

To check the validity of this assumption, axial dispersion will be included in the energy equation here. Results will first be compared with experimental data to check the model validity. Then results will be compared with the case with no axial dispersion. Heat transfer in the thermally developing region will be shown to be influenced by axial dispersion in a certain flow regime ($\mathrm{Pe} < 10$).

Contributed by the Heat Transfer Division and presented at the ASME Winter Annual Meeting, Atlanta, Georgia, December 1–6, 1991. Manuscript received by the Heat Transfer Division March 1992; revision received July 1994. Keywords: Environmental Heat Transfer, Numerical Methods, Porous Media. Associate Technical Editor: C. E. Hickox, Jr.

Governing Equations

The flow geometry under investigation here is shown in Fig. 1. Flow enters the tube at a uniform temperature T_{in}, the wall temperature is kept constant at another temperature T_w. The volume-averaged governing equations for an incompressible fluid are

$$\nabla \cdot \hat{V} = 0 \tag{1}$$

$$-\nabla P + \rho \hat{g} - \mu \frac{\hat{V}}{\gamma} - \rho \frac{F}{\gamma} |\hat{V}| \hat{V} + \mu \nabla^2 \hat{V} = 0 \tag{2}$$

$$(\rho C_p)_0 \frac{\partial T}{\partial t} + (\rho C_p)_f \hat{V} \cdot \nabla T = \nabla \cdot (k_e \nabla T) \tag{3}$$

The permeability γ and inertia resistance coefficient F were determined empirically by Ergun (1952) for sphere-pac beds to be

$$\gamma = \frac{d^2 \epsilon^3}{150(1-\epsilon)^2}, \quad F = \frac{1.75d}{150(1-\epsilon)} \tag{4}$$

It should be noted that these quantities depend on the porosity of the packed bed, which is not uniform across the tube. Experimental measurements of Benenati and Brosilow (1962) and Roblee et al. (1958) showed that the porosity of a sphere-pac bed varies sinusoidally from the free-stream value (ϵ_∞) of 0.4 to a value of 1 at solid boundaries. Hunt and Tien (1988) have suggested the following relationship for porosity variation in sphere-pac beds:

$$\epsilon = \epsilon_\infty \left[1 + 1.5 \exp\left(-\frac{6y}{d} \right) \right] \tag{5}$$

where y is the distance from side walls. This porosity variation allows for channeling of flow near solid boundaries. After combining the gravity term with the hydrostatic pressure in the momentum equation, one can nondimensionalize the governing equations using R_t, ν/R_t, $(T - T_w)/(T_{in} - T_w)$, $\rho\nu^2/R_t^2$ for length, velocity, temperature, and pressure, respectively, to get

$$\frac{\partial u'}{\partial z'} = 0 \tag{6}$$

$$-\frac{\partial P'}{\partial z'} - \frac{1}{\mathrm{Da}} u' - \omega |u'| u' + \frac{1}{\epsilon} \frac{1}{r'} \frac{\partial}{\partial r'} \left(r' \frac{\partial u'}{\partial r'} \right) = 0 \tag{7}$$

$$\Omega \, \mathrm{Pr}_f \frac{\partial T'}{\partial t'} + \mathrm{Pr}_f u' \frac{\partial T'}{\partial z'} = \frac{1}{r'} \frac{\partial}{\partial r'} \left(r' k_r' \frac{\partial T'}{\partial r'} \right) + \frac{\partial}{\partial z'} \left(k_a' \frac{\partial T'}{\partial z'} \right) \tag{8}$$

The primes denote dimensionless quantities. The subscripts r and a denote radial and axial direction, respectively. The velocity profile inside the tube is assumed to be hydrodynamically developed because studies such as Vafai (1984) have shown the size of entrance region for a packed bed to be very small. Within the solution domain, the flow is initially thermally developing and becomes nearly thermally developed with axial distance. The tube is long enough for the flow to become close enough to being thermally developed for the assumption of a zero axial temperature gradient to have little effect on the inlet region where axial dispersion is important. This was tested by increasing the computational length of the tube until no effect on the inlet region was found. The M/R_t found that met this criterion was about 40 and that used in the computation was 45. The following boundary conditions were utilized:

$$T' = 1 \quad @ \quad z' = 0$$
$$\frac{\partial T'}{\partial z'} = 0 \quad @ \quad z' = \frac{M}{R_t}$$
$$\frac{\partial T'}{\partial r'} = 0 \quad @ \quad r' = 0$$
$$T' = 0 \quad @ \quad r' = 1 \qquad (9)$$

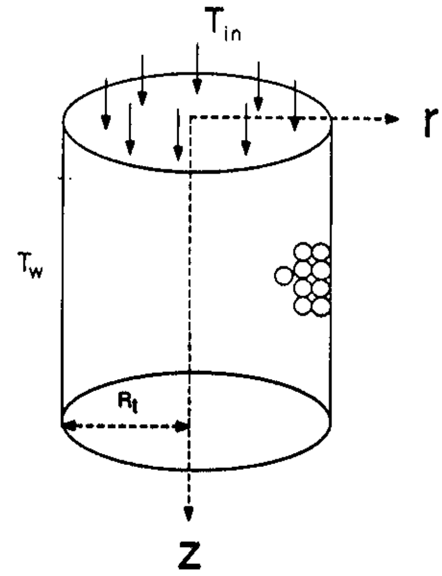

Fig. 1 Forced convection in a packed tube

Radial and Axial Dispersion

Results from experiments of Levec and Carbonell (1985) and Yagi et al. (1960) show the effective thermal conductivities in the axial and radial directions to be different. Both studies suggest the axial component is larger than the radial component. Physically, this makes sense because interstitial velocities in the axial direction are larger than the interstitial velocities in the radial direction. To account for this anisotropy, different models will be used at each direction. In the radial direction, a modified version of the model by Cheng and Vortmeyer (1988) will be utilized. They suggest a linear relation between the dispersive component and the filtration velocity:

$$k_r' = \frac{k_0}{k_f} + D_T \xi \, \mathrm{Pr}_f \, \mathrm{Re} \qquad (10)$$

where

$$\xi = \begin{cases} \left(\dfrac{y}{\tau d}\right)^m & \text{if } 0 \le y \le \tau d \\ 1 & \text{if } y > \tau d \end{cases} \qquad (11)$$

Cheng and Vortmeyer (1988) suggest that the magnitudes of D_T, τ, and m are 0.25, 2.5 and 1 correspondingly. Since their model was derived assuming the flow has no inertia, it will be modified here by choosing D_T to be 0.14 so that the results match the experimental data when flow has inertia. The conductivity k_0 is the effective medium conductivity when the fluid is stagnant. Its value is determined by using the two-dimensional unit cell model developed by Adnani et al. (1989). ξ is a wall function that dampens hydrodynamic dispersion near solid boundaries. It is included here because, as the porosity is increased near solid boundaries, the path of fluid particles becomes less tortuous and dispersion becomes weaker. Combining ξ and Re yields

$$\xi \, \mathrm{Re} = \begin{cases} \dfrac{y}{\tau d}\dfrac{ud}{\upsilon} = \dfrac{u}{\upsilon}\left(\dfrac{y}{\tau}\right) & 0 \le y \le \tau d \\ \dfrac{u}{\upsilon}(d) & y > \tau d \end{cases} \qquad (12)$$

Nomenclature

C_p = specific heat at constant pressure
d = diameter of particles in a packed bed
Da = Darcy number = γ/L^2
D_T = empirical coefficient of dispersivity (Eq. (10))
F = inertia resistance coefficient (Eq. (4))
g = gravitational constant
h = local heat transfer coefficient (Eq. (16))
k = thermal conductivity
m = parameter in Eq. (11)
M = tube length
Nu = bulk Nusselt number (Eq. (15))
P = pressure
Pe = Peclet number = $\mathrm{Pr}_f \times \mathrm{Re}$
Pr_f = fluid Prandtl number = $(\mu C_p)_f/k_f$
r = radial coordinate
R_t = tube radius
Re = particle Reynolds number = ud/υ
T = temperature
t = time
u, v, w = velocity components
$\vec{V}$ = velocity vector
x, y, z = coordinate axes
γ = permeability (Eq. (4))
ϵ = porosity
μ = dynamic viscosity
ν = kinematic viscosity
ξ = wall damping parameter (Eq. (11))
ρ = density
τ = empirical damping parameter (Eq. (11))
ω = dimensionless inertial coefficient = FL/γ
Ω = $(\rho C_p)_0/(\rho C_p)_f$

Subscripts

a = axial
avg = averaged in the radial direction
b = bulk value
e = effective value with flow
f = fluid
in = inlet condition
r = radial
w = wall
wi = with axial dispersion
wo = without axial dispersion
0 = effective value with stagnant fluid
∞ = far away from walls (free stream)

Superscripts

$'$ = dimensionless

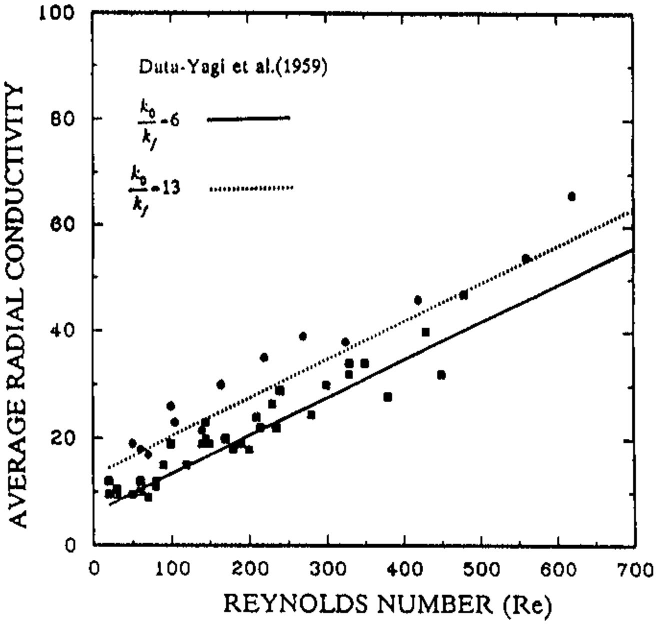

Fig. 2 Comparison of effective conductivity with data of Yagi and Wakao (1959)

The term inside the parentheses can be regarded as a mixing length. In the core region this mixing length is equivalent to the bead diameter because dispersivity is proportional to the bead diameter. Near the walls, mixing length has a value smaller than d because the path of fluid particles is less tortuous. To account for this variation, the mixing length is assumed to vary linearly from 0 at the wall to d at 2.5 particle diameters away from the wall. Note that near the wall, the value of the mixing length is bounded between 0 and d; therefore, even in this region the mixing length still depends on the particle size in a porous medium.

To estimate the axial dispersion coefficient (k_a) a modified version of the model suggested by Georgiadis (1987) will be used

$$k_a' = \frac{k_0}{k_f} + \frac{0.43}{1-\epsilon_\infty}\xi\, \mathrm{Pr}_f \mathrm{Re} \tag{13}$$

This model is modified to account for damping of hydrodynamic dispersion near solid walls by introducing the function ξ. Although this is done in an ad-hoc fashion, one must keep in mind that the same idea has been applied successfully to the radial component. The primes (denoting dimensionless quantities) will be dropped from here on for simplicity.

Method of Solution

As an approximation, material properties for the fluid and solid phases will be assumed constant here. This is a reasonable assumption if the temperature and pressure do not change significantly inside the tube and the properties are evaluated at an average pressure and temperature. To model the sharp gradients and the channeling of flow near solid surfaces, a nonuniform grid is formed in the radial direction. For most calculations approximately 50 points were used in the radial direction and 600 points in the axial direction. In the radial direction 30 grid points were positioned within 4 bead diameters from the wall and the rest were spaced equally inside the tube. The momentum equation (Eq. (7)) is discretized in the radial direction, and is solved in an iterative fashion after specifying the axial pressure gradient.

Once the material properties and gas pressure are known, the effective medium conductivity with stagnant gas (k_0) can be determined from the unit cell model developed by Adnani et al. (1989). After solving the momentum equation and determining the velocity field, one can calculate the effective conductivities (k_a, k_r) from Eqs. (10) and (13). Note that these quantities change in the radial direction (r) but, because the flow is assumed to be hydrodynamically developed, there is no variation of conductivity in the axial direction (z). The energy equation (Eq. (8)) is solved using a two-dimensional time-dependent ADI scheme. The advective term in the energy equation was discretized using upwind differencing to avoid problems at high Peclet numbers.

Comparison With Experimental Results

It was mentioned earlier that the radial conductivity model of Cheng and Vortmeyer (1988) was derived after assuming the flow has no inertia. Although this assumption is reasonable for cases where Re is less than 10, it is not so good at higher flow rates (see Georgiadis, 1987). Therefore, the empirical coefficient (D_T) of Cheng and Vortmeyer (1988) will be modified here so that good agreement with experimental results is obtained when flow has inertia.

To demonstrate the adequacy of the thermal model, the momentum and energy equations were integrated for the flow conditions corresponding to the experimental measurements in air by Yagi and Wakao (1959). Their data show some scattering at all Re (Fig. 2); this requires an explanation. Yagi and Wakao (1959) used various types of particle in their experiments. Some of these (i.e., cement clinkers) are not perfectly spherical. Additionally, results for different Re were obtained by either changing the flow rate or by changing the particle size. This means effective medium properties may have been changed, inadvertently, during the experiments. In spite of this, the predicted average conductivity (k_{avg}) defined by

$$k_{avg} = \frac{\int_0^1 2\pi k_r r dr}{\int_0^1 2\pi r dr} \tag{14}$$

is well within the experimental uncertainty range of Yagi and Wakao (1959) when D_T is chosen to be 0.14.

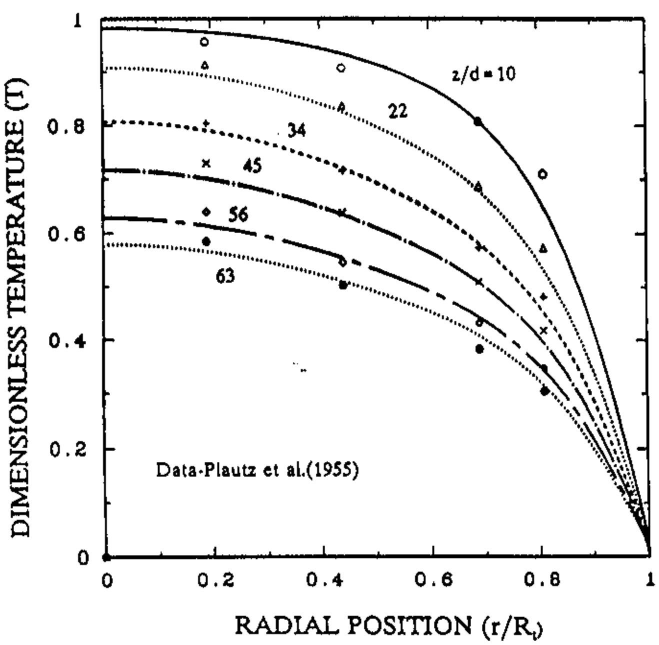

Fig. 3 Comparison of temperature profile with data of Plautz and Johnstone (1955)

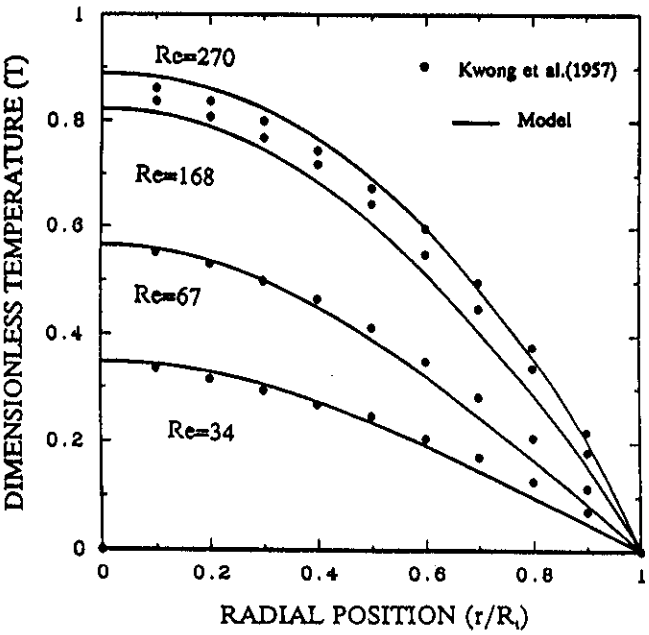

Fig. 4 Comparison of temperature profile with data of Kwong and Smith (1957)

A better set of data was obtained from the experiments of Plautz and Johnstone (1955). They performed their experiments with spherical glass particles at various air flow rates. Figure 3 shows the model prediction and the experimental results at different axial locations. Excellent agreements are obtained at all locations. Note that Re for this case is approximately 1000, meaning dispersion is the dominant mechanism influencing the heat transfer. To check the validity of our model at other Re, results were compared with the data of Kwong and Smith (1957). They were actually the first people who suggested that the radial conductivity is nonuniform across the tube. Figure 4 shows the model predictions and Kwong and Smith's data (1957) for a range of Re. All of the data were taken at 26 bead diameters downstream of the inlet. Considering the fact that the experimental uncertainty in these measurements was roughly ±10 percent, excellent agreement is obtained at all Re.

Influence of Axial Dispersion

The objective in the previous section was to check the validity of the thermal conductivity models. It has been known for a long time that the axial diffusion term in the equivalent of this problem in a nonporous tube can be neglected for most cases (the only exception is liquid metals at low Pe). In porous media, however, the axial dispersion term depends on the filtration velocity. This means that neglecting the axial dispersion term might not be a correct assumption at all Pe. In this section, we test the validity of this hypothesis. We consider flow at several Pe to see whether the axial advective term is always larger than the axial dispersive term. In order to carry out a nondimensional analysis, ratio of Nu with axial dispersion over Nu without axial dispersion (Nu_{wi}/Nu_{wo}) will be plotted as a function of axial position. Nu is defined to be

$$\mathrm{Nu} = \frac{2hR_t}{k_f} \tag{15}$$

where h is the local heat transfer coefficient

$$h = \frac{1}{T_b - T_w}\left(k_r \frac{\partial T}{\partial r}\right)_w \tag{16}$$

and T_b is the bulk mean temperature

$$T_b = \frac{2\pi \int_0^1 uTrdr}{2\pi \int_0^1 urdr} \tag{17}$$

Figure 5 shows the results in the thermally developing region of the tube for Pe ranging from 0.7 to 14. Note that axial dispersion enhances the heat transfer (increased Nu) in the thermally developing region of the pipe. This effect disappears at some location downstream, and the location depends on Pe. It can be observed that at low Pe (Pe < 10), the axial dispersion term does play a role on determining the heat transfer in the pipe. As Pe is increased, the advective term in the axial direction becomes larger and the presence of axial dispersion does not affect the results significantly.

Conclusions

The influence of axial dispersion on heat transfer in a packed tube was investigated by incorporating a term to represent the axial dispersion in the energy equation. Previous studies in this area neglect axial dispersion in all flow regimes. Non-Darcian effects, i.e., flow inertia, porosity variation near walls, and dispersion damping near walls were also incorporated in the governing equations. Dispersion was assumed to be anisotropic in the radial and axial directions as suggested by the experimental evidence in the literature. Results in the radial direction were shown to be in good agreement with data of Yagi and Wakao (1959), and the accuracy of the axial dispersion model has been tested by Georgiadis (1987). Excellent agreement with the data of Plautz and Johnstone (1955) and Kwong and Smith (1957) was achieved when the combined axial and radial dispersivity models were used.

The analysis in this paper was done to determine whether the axial dispersion can be neglected at all Pe while studying convective heat transfer processes in porous media. It was shown that heat transfer results for Pe < 10 can be underestimated if axial dispersion is not included in the analysis. The smaller the Pe, the larger the influence of axial dispersion. A set of dimensionless graphs is developed to show the importance of axial dispersion at various Pe. For Pe > 10 the axial advective term

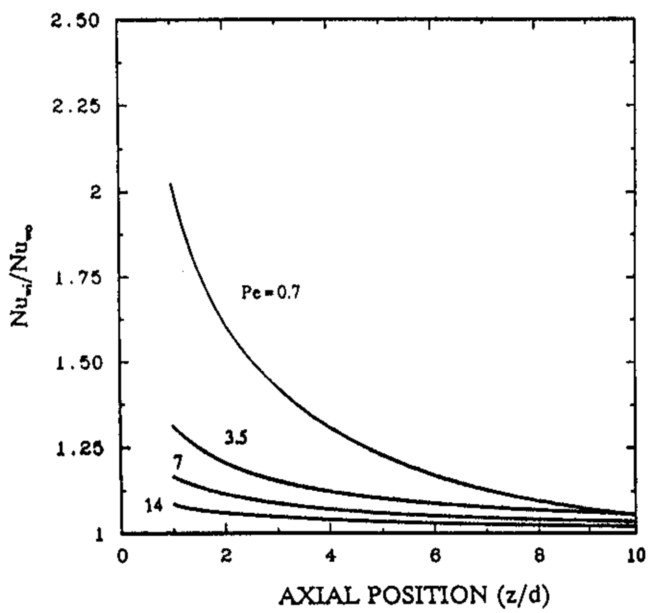

Fig. 5 Influence of axial dispersion on axial heat transfer

becomes large enough that axial dispersion can be neglected without affecting the result in a significant manner. Therefore, previous studies in this area are correct only in the flow regime Pe > 10. At smaller Pe, one must either include axial dispersion in the analysis or use information similar to what was shown in Fig. 5 to correct for the heat transfer results.

Acknowledgments

This work was supported by the U.S. Department of Energy under contracts #DE-FG03-86ER52123 and #DE-FG03-86ER14033. We would like to thank one of the reviewers for calling our attention to the interesting and informative paper by Sozen and Vafai (1993). Unfortunately, it was called to our attention too late in the review process to exploit fully what it contained.

References

Adnani, P., Raffray, A. R., Abdou, M. A., and Catton, I., 1989, "Modeling of Effective Thermal Conductivity for a Packed Bed," Report No. UCLA-FNT-29, University of California, Los Angeles.

Benenati, R. E., and Brosilow, C. B., 1962, "Void Fraction Distribution in Beds of Spheres," *AIChE Journal*, Vol. 8, No. 3, pp. 359–361.

Bunnell, D. G., Irvin, H. B., Olson, R. W., and Smith, J. M., 1949, "Effective Thermal Conductivities in Gas–Solid Systems," *Ind. Eng. Chem.*, Vol. 41, No. 9, pp. 1977–1981.

Cheng, P., and Vortmeyer, D., 1988, "Transverse Thermal Dispersion and Wall Channelling in a Packed Bed With Forced Convective Flow," *Chem. Eng. Sci.*, Vol. 43, No. 9, 2523–2532.

Coberly, C. A., and Marshall, W. R., 1951, "Temperature Gradients in Gas Streams Flowing Through Fixed Granular Beds," *Chem. Eng. Prog.*, Vol. 47, No. 3, pp. 141–150.

Ergun, S., 1952, "Fluid Flow Through Packed Columns," *Chem. Engng. Prog.*, Vol. 48, No. 2, pp. 89–94.

Georgiadis, J. G., 1987, "Nonlinear Convective Transport in Packed Beds," Ph.D. Dissertation, University of California, Los Angeles, CA.

Hunt, M. L., and Tien, C. L., 1988, "Non-Darcian Convection in Cylindrical Packed Beds," ASME JOURNAL OF HEAT TRANSFER, Vol. 110, pp. 378–384.

Kwong, S. S., and Smith, J. M., 1957, "Radial Heat Transfer in Packed Beds," *Ind. and Eng. Chem.*, Vol. 49, No. 5, pp. 894–903.

Levec, J., and Carbonell, R. G., 1985, "Longitudinal and Lateral Thermal Dispersion in Packed Beds, Part II: Comparison Between Theory and Experiment," *AIChE Journal*, Vol. 31, No. 4, pp. 591–602.

Plautz, D. A., and Johnstone, H. F., 1955, "Heat and Mass Transfer in Packed Beds," *AIChE Journal*, Vol. 1, No. 2, pp. 193–199.

Roblee, L. H. S., Baird, R. M., and Tierney, J. W., 1958, "Radial Porosity Variations in Packed Beds," *AIChE Journal*, Vol. 4, pp. 460–464.

Sozen, X. X., and Vafai, K., 1993, "Longitudinal Heat Dispersion in Porous Beds With Real Gas Flow," *AIAA Journal of Thermophysics and Heat Transfer*, Vol. 7, No. 1.

Vafai, K., 1984, "Convective Flow and Heat Transfer in Variable-Porosity Media," *J. Fluid Mech.*, Vol. 147, pp. 233–259.

Yagi, S., and Wakao, N., 1959, "Heat and Mass Transfer From Wall to Fluid in Packed Beds," *AIChE Journal*, Vol. 5, No. 1, pp. 79–85.

Yagi, S., and Kunii, D., 1960, "Studies on Heat Transfer Near Wall Surface in Packed Beds," *AIChE Journal*, Vol. 6, No. 1, pp. 97–104.

Yagi, S., Kunii, D., and Wakao, N., 1960, "Studies on Axial Effective Thermal Conductivities in Packed Beds," *AIChE Journal*, Vol. 6, No. 4, pp. 543–546.